University of Florida

Development of Low-Cost CIGS Thin Film Hot Carrier Solar Cells

PI: Gijs Bosman **Co-PI:** Tim Anderson
Students: Yige Hu, PhD.

Description: PV has entered into a period of record growth. Most of the current production is based on crystalline Si technology. However, there are fundamental limits to the ultimate Si costs that may inhibit it from achieving the desired level of contribution to worldwide energy production. In contrast, thin-film PV technology can reach the desired outcome due to fast deposition rates and lower cost. Our study is focused on hot carrier solar cells for cell conversion efficiency improvement in a low cost, high throughput CIGS system. The rapid thermalizaton loss of hot photoexcited carriers interacting with the lattice can potentially be reduced through phonon engineering in the absorber layer; the subsequent extraction of the hot carriers may be realized through device engineering of energy selective contacts.

Budget: $ 126,112.00
Universities: UF

Progress Summary

Hot carrier solar cells allow hot carriers to be collected before energy is lost to the lattice. This ultimately leads to a higher open circuit voltage since the average energy of the collected electron is greater than the band gap energy. It also leads to a higher short circuit current, leading to an overall greatly improved efficiency.

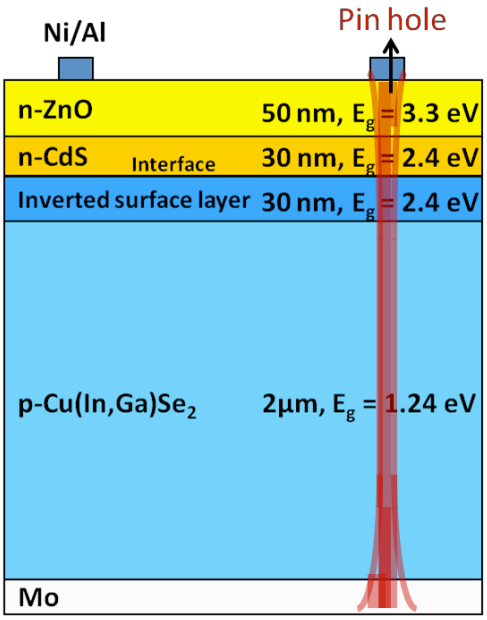

FIGURE 1 CIGS PIN HOLE STRUCTURE

Photocurrent measurements as a function of applied bias were carried out on fabricated CIGS solar cell structures to characterize the hot carrier effect. In a preliminary experiment the CIGS cell is exposed by LED light of wave length 365nm, 455nm, 630nm and 740nm, respectively. The incident photon energy defines the initial hot carrier energy. The resulting current shows a different bias dependency with respect to high energy carriers and low energy carriers. A relationship between the photocurrent and initial hot carrier energy is being formulated from which the relative density of hot electrons and its effect on cell operation can be determined from measured current voltage data.

A study of the reverse bias dark JV characteristic helps in the separation of hot carrier effects from other device phenomena. The commonly used dark current model: $J_{dark} = J_0\left[e^{\frac{q(V-IR_s)}{nk_BT}} - 1\right]$ cannot explain the linear characteristic at low reverse bias and superlinear characteristic at high reverse bias of the CIGS solar cell. Space charge limited current (SCLC) via pinholes in the ZnO and CdS layers

consisting of a metal-CIGS-molybdenum structure (Figure1) is proposed as contributing to the reverse bias leakage current [1].

The SCLC model helps to better understand the dark current and gives a baseline for separating the photocurrent contribution from dark current components in the CIGS cell. Therefore our hope is that photon induced hot carrier effects can be uncovered and demonstrated.

Annual Progress Report

The focus of this period is studying the dark IV characteristic of CIGS solar cells to extract photocurrent from the measured total current.

The dark current density is commonly modeled as $J_{dark} = J_0\left[e^{\frac{q(V-IR_s)}{nk_BT}} - 1\right]$ where $J_0=J_{01}+J_{02}$ is the diode saturation current density. $J_{01} = q[\frac{D_n n_{p0}}{L_n} + \frac{D_p p_{n0}}{L_p}]$ is the diffusion related component and $J_{02} = q\frac{n_i}{2}Wv_{th}N_t\sigma$ is the trap assisted generation-recombination related component. J_{02} dominates via generation the reverse dark current density for a non-ideal device. The depletion width $W \propto \sqrt{V_{bi}+V}$, therefore J_{02} follows a square root dependency of the bias. However, the experimental dark current density in CIGS solar cells reported in the literature is observed having a linear characteristic at low reverse bias and superlinear at high reverse bias. Mechanical scratches are proposed to explain the linear behavior since the reverse current increases dramatically with the increase of the load of scratches and the reverse current varies linearly over $1/T^{1/4}$ [2]. In our previous experiment on the 19% efficient "champion cell", the reverse dark current density (Figure 2) shows neither square root nor linear bias dependence. The generation related component and "scratch effect" are not able to exhibit the characteristic. Space charge limited current (SCLC) via pinholes in the ZnO and CdS layers consisting of a metal-CIGS-molybdenum structure is proposed as contributing to the reverse bias leakage current [1].

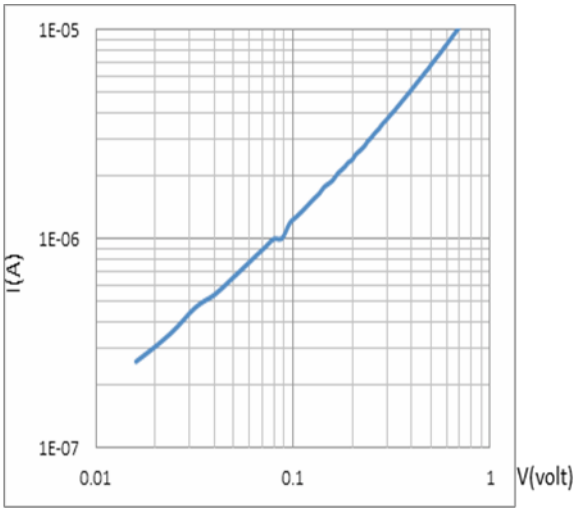

FIGURE 2 CIGS DARK IV REVERSE BIAS CHARACTERISTIC

Ohm's Law $J = q\mu n_0\frac{V}{L}$ dominates at low applied voltage, where n_0 is the electron density from thermal generation. When the electrode injects carriers exceeding the number of thermal carriers, the linear relation of the current and voltage no longer holds. The resulting SCLC is proportional to the square of the voltage[1]. It is expressed as $J = q\mu n_s\frac{V}{L} = q\mu\frac{\epsilon_0\epsilon_r V}{qL^2}\cdot\frac{V}{L} = \mu\frac{\epsilon_0\epsilon_r V^2}{L^3}$. The crossover voltage V_T, where the current transitions from Ohm's law to the square law, can be calculated as $V_T = \frac{L^2 qn_0}{\epsilon_0\epsilon_r}$ [Eq. 1.]

A MEDICI simulation is carried out to check if the software can handle SCLC phenomena where specifically the contact boundary conditions play an important role. The heavily doped n-type CIGS, modeling a metallic pinhole shorting the contact to the absorber layer, provides excess electrons for injecting into the lightly doped p-type CIGS. The dark current density versus voltage is shown in Figure 3. The current density follows ohm's law at low bias and the square law in the high bias regime, as shown

FIGURE 3 MEDICI SIMULATED CIGS ELECTRON DENSITY PROFILE

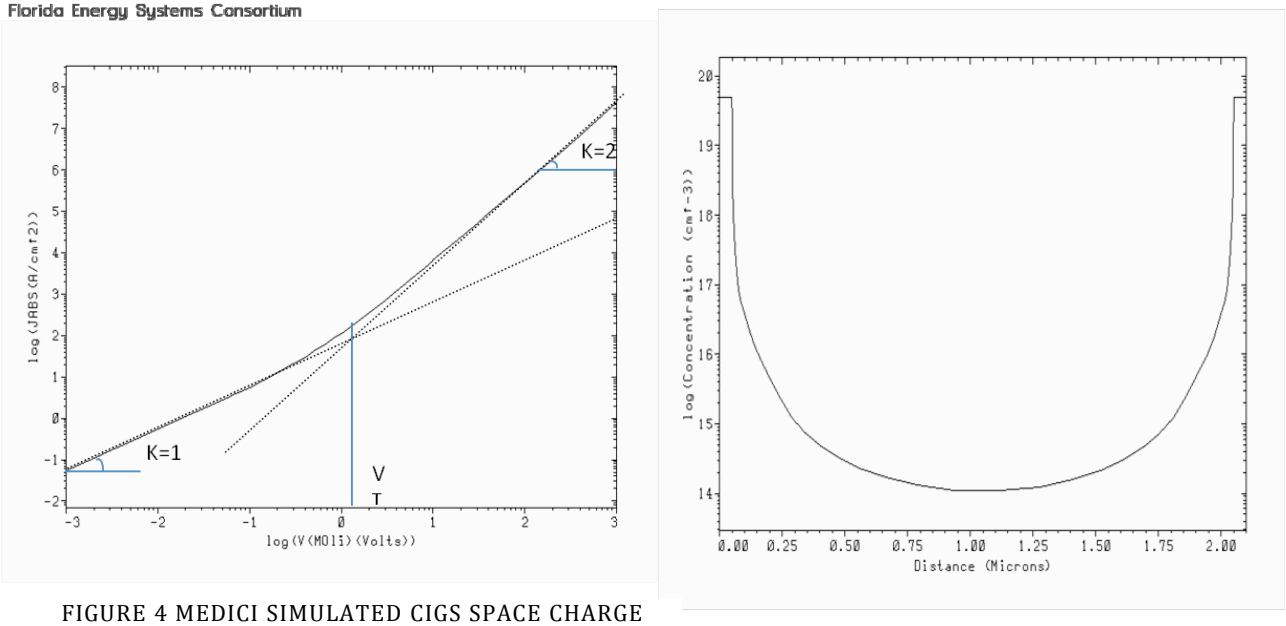

FIGURE 4 MEDICI SIMULATED CIGS SPACE CHARGE LIMIT CURRENT

by the extrapolation lines with log slopes of 1 and 2, respectively. The doping density of the p-type CIGS is 6×10^{11}/cm^2. At V=10^{-3} volts, the ohm's law current density is calculated: $j = q\mu_p p\frac{V}{L} = qN_a\frac{V}{L} = 1.44\times10^{-4}A/cm^2$. The plot in Figure 3 reads a current density of 5×10^{-2} A/cm^2 at the same voltage. The increased current density comes from the fact that the carrier density of the lightly doped p-region is converted to n-type by the adjacent heavily doped n^+ regions. The electron density is plotted in Figure 4. The heavily doped n^+ contacts make the effective carrier density between the contacts to become 10^{14}/cm^3 and the effective distance between contacts reduces to 1μm due to diffusion. The current density is then calculated as $q\mu_n n\frac{V}{L} = 4\times10^{-2}A/cm^2$.The crossover voltage V_T equals 1.2V as calculated from Eq. 1. In Figure 3, the point at where the extrapolated lines cross agrees with this value. At the crossover voltage, the total current density is twice the corresponding ohmic current density, since it is where the SCLC from the excess carriers equals the ohmic current from the thermal carriers. The total current density is the sum of these two components.

In a CIGS solar cell, the contact metal may penetrate the thin layers of ZnO and CdS causing "pinholes" that are essentially extensions of the metal electrode contacting the CIGS directly. In addition the CIGS layer may have regions with low densities of acceptor sites. If the pinholes contact an area of low-carrier density in the CIGS they form a SCLC structure, because the low-carrier density causes the crossover voltage to occur sooner and the metal electrodes are abundant electron carrier sources. Pinhole current is a parasitic loss in a CIGS device. The total current is expressed as a sum of current through the pinholes and current through the rest

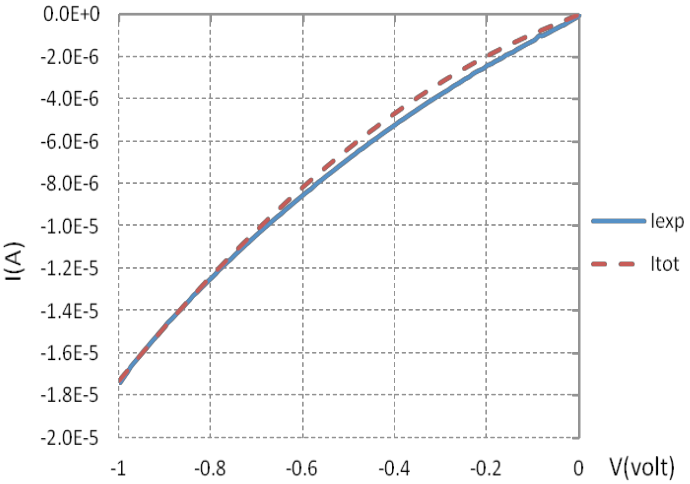

FIGURE 5 SPACE CHARGE LIMITED CURRENT MATCHING WITH THE MEASURED CIGS REVERSE BIASED DARK CURRENT DENSITY

of the device: $I_{total}=J_{SCLC}\times A_{SCLC}+J_{solar}\times A_{solar}$, where A_{SCLC} and A_{solar} are the overall effective pinhole area and the solar cell area, respectively. Under reverse bias, the total current is dominated by the SCLC giving weak voltage dependence. As the voltage increases in forward bias, the solar current increases exponentially and eventually dominates the total current. The SCLC matching with the CIGS "champion cell" dark current versus reverse bias voltage is shown in Figure 5, where measured reverse bias dark current is compared to current simulated via the pin-hole model. The pinhole area is calculated by $A_{SCLC}=I_{total}/J_{SCLC}$ in the reverse bias section. I_{total} is the experiment dark current and J_{SCLC} is obtained by the MEDICI program. The calculated effective pinhole area is about $0.147\mu m^2$, which makes up only $1/10^7$ of the solar cell contact area. The pinhole current is calculated from the simulated pinhole current flux multiplied by the pin hole area plus the dark current density simulated by the MEDICI program. Figure 5 shows that there is a good match between the experiment and the model.

[1] M.A.Lampert, "Universality of non-Ohmic shunt leakage in thin-film solar cells," *Journal of Applied Physics*, vol. 108, Dec. 2010, pp. 124509-124509-10
[2] O. Breitenstein, J. Bauer, A. Lotnyk, and J. Wagner, "Defect induced non-ideal dark characteristics of solar cells," *Superlattices and Microstructures*, vol. 45, 2009, pp. 182 – 189